Dielectric properties of DWCNTs/silicone nanocomposites under AC field: influence of the polymer matrix

Iryna Sulym[1,2,*], Hugo Luis[1], Emmanuel Flahaut[3], Yann Borjon-Piron[3], Marie-Laure Locatelli[1], Zarel Valdez-Nava[1]

[1] Université de Toulouse, Toulouse INP, CNRS, LAPLACE, Toulouse, France

[2] Chuiko Institute of Surface Chemistry of NASU, Kyiv, Ukraine

[3] CIRIMAT, Université de Toulouse, Toulouse INP, CNRS, Toulouse, France

*sulym@laplace.univ-tlse.fr

ABSTRACT - The impact of adding an amount of PDMS-20 into the silicone matrix of silicone-based composites containing double-walled carbon nanotubes (DWCNTs) on their electrical and morphological properties has been studied. Two series of elastomeric polymer nanocomposites were developed, consisting of Sylgard 184 with- or without a PDMS-20 part, both filled with a small content of DWCNTs (0.005 – 2.5 wt.%). The AC electrical conductivity (σ_{AC}) of both silicone-based nanocomposites increased with increasing the wt.% content of DWCNTs. The electrical percolation threshold for both series was determined below 0.1 wt.% of DWCNTs. We have shown that the addition of PDMS-20 improves the conductivity in the whole frequency range. We also found that adding PDMS-20 affects the morphology of the resulting DWCNTs/silicone nanocomposites. The lower viscosity of the polymer matrix mixture resulting from the addition of a PDMS-20 portion is supposed to explain the obtained results, providing better dispersion of DWCNTs particles.

Keywords — double-walled carbon nanotubes, SYLGARD™ 184, PDMS-20, DWCNTs/silicone nanocomposites, electrical properties, percolation threshold, SEM.

1. INTRODUCTION

Today, all of materials science has been transformed by composite materials. In the constant search for better performance, researchers strive to create either improved traditional materials or completely new materials [1], [2]. Multiphase materials consisting of two or more components with different properties and distinct boundaries between the components are called composite materials [2]. More precisely, the main components of the composite materials are matrices and additives (fillers). They include three categories according to their main matrix: ceramic composites, metal composites, and polymer composites [2], [3]. To date, polymer composites are widely used in various industries due to their reasonable price, straightforward synthesis, and outstanding properties [4]. The polymer matrix can be thermoplastic, thermosetting and/or elastomeric [2]. The choice of matrix depends on the intended use of the polymer composite material. Silicone rubbers, also known as polysiloxanes, are the main polymeric insulating materials used in aerospace, automotive, electronic, electrical and other industries [5], [6], [7] due to their excellent properties such as softness, chemical stability, high heat resistance and good electrical insulation [5]. Many different types of fillers, namely carbon black, calcium carbonate, kaolin, zeolites, glass fibers, and talc in the micrometer size range, have been added to silicones to provide enhanced final product properties [8]. However, this improvement is only achieved at high filler concentrations, which leads to increased material viscosity and therefore processing problems. In recent years, it has been observed that the incorporation of only a small amount of particles in nanoscale range (1–100 nm) significantly improved the properties of virgin polymers without affecting their processability [9]. In this sense, carbon nanotubes (CNTs) are among the most studied electrically conductive carbon fillers used in polymer composites due to their ability to significantly enhance electrical conductivity even in small quantities [9], [10], [11], [12]. CNTs are mainly classified into two types: single-walled carbon nanotubes (SWCNTs) and multi-walled carbon nanotubes (MWCNTs), double-walled carbon nanotubes (DWCNTs) sitting at the interface between the two. In addition, in the case of electrical insulating materials (including silicones), they remain dielectric materials with the incorporation of conductive CNTs below a certain content. As the concentration of CNTs in a nanocomposite increases, the specific volume fraction corresponding to a transition from insulator to conductor is called the percolation threshold. The electrical percolation threshold (EPC) of a polymer nanocomposite can be influenced by several factors, including synthesis method, filler's intrinsic properties and the dispersion/distribution of the nanofiller within the polymer matrix [11], [13]. In the case of CNTs-silicone composites, the properties of SWCNTs and MWCNTs are widely described in the literature, while the specific case of DWCNTs remains much less explored [14]. A DWCNTs are composed of two concentric carbon shells. Their unique combination of high aspect ratio, compared to MWCNTs, and better electrical properties than SWCNTs [15], makes them excellent candidates for improving electron transport properties at very low concentrations.

This study reports the fabrication and the comparative study of two series of low-filler loading (0.005 – 2.5 wt.%) DWCNTs/silicone nanocomposites, differing by the addition of a low viscosity silicone fluid in the elaboration process of one of them. The aim is to investigate the effect of the polymer matrix on the DWCNTs dispersibility, and on the electrical

conductivity as well as on the electrical percolation threshold of the resulting polymer nanocomposites.

2. Experimental procedure

2.1. Materials

DWCNTs (with a mean outer diameter of 2 nm, and carbon purity superior to 95 %) were synthesized by catalytic chemical vapor deposition (CCVD) using $Mg_{0.99}Co_{0.0075}Mo_{0.0025}O$ catalyst as previously described [16]. Here, two types of siloxanes were used: (***i***) the 2-component optically transparent silicone elastomer hereafter named S184 (SYLGARD™ 184, Dow Corning, Germany) (base elastomer (Part A) and curing agent (Part B) with viscosity 3500 cSt (mixed part A + part B); (***ii***) the trimethyl-terminated silicone oil poly(dimethylsiloxane) (PDMS) with low viscosity (20 cSt) termed as PDMS-20 (Sigma-Aldrich, Germany). *n*-Hexane solvent (Alfa Aesar (Kandel, Germany), HPLC grade with >95 % purity), was used to enhance DWCNTs dispersion.

2.2. Preparation of DWCNTs/silicone nanocomposites

One series of DWCNTs/silicone nanocomposites with the DWCNTs concentrations (0 / 0.005 / 0.01 / 0.03 / 0.05 / 0.1 / 0.5 / 1.0 / 1.5 / 2.0 / 2.5 % by weight) (hereinafter referred to as xDWCNTs/S184 + PDMS-20) was fabricated according to the following optimized procedure, which is summarized in Fig. 1.

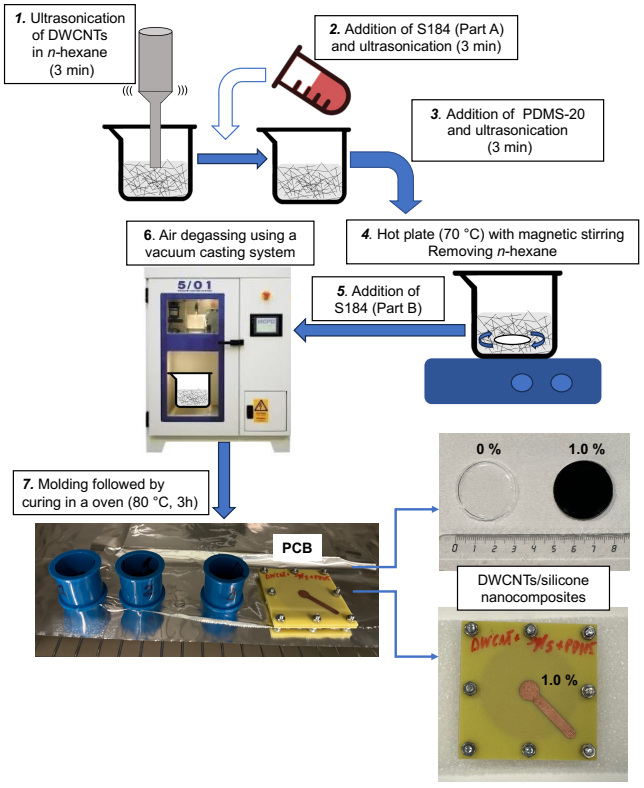

Fig. 1. Schematic diagram of the DWCNTs/silicone nanocomposites preparation steps.

In the first step (Fig. 1 (***1***)), the specified amount of DWCNTs was dispersed for 3 min in *n*-hexane (20 ml) using a sonication probe operated at a 40 % and at a frequency of 20 kHz. During the ultrasonic process, the beaker with DWCNTs/*n*-hexane solution was immersed in an ice bath. Subsequently, S184 (part A) was added to the DWCNTs/*n*-hexane suspension and ultrasonicated for 3 min (***2***). To achieve a more homogeneous mixture, low-viscosity silicone fluid PDMS-20 was added followed by 3 min of ultrasonication (***3***). After evaporation of *n*-hexane on a hot plate at 70 °C (20 min) using a magnetic stirrer at 200 rpm (***4***), S184 (part B) was added (part A:part B ratio was 10:1) and the mixture was vigorously stirred manually (***5***). A vacuum casting system was then used (***6***) to degas the mixture. The final blend was cast into cylindrical molds (30 mm in diameter) for morphological analysis as well as transferred into rigid sandwich structures for electrical tests, and then cured in an oven at 80 °C for 3 h (***7***). Samples with the same DWCNTs content, filled with S184 silicone but without PDMS-20 addition (named as xDWCNTs/S184 in the following), were also prepared (same protocol as presented on Fig. 1 *avoiding step* ***3***). Moreover, samples of the two neat silicone matrices (S184 + PDMS-20 and S184) were elaborated as well. The thickness of the polymer samples casted into cylindrical molds was approximately 1 mm.

2.3. Characterization of DWCNTs/silicone nanocomposites

To obtain a detailed profile of the frequency-dependent electrical properties in alternating current (AC), the broadband dielectric spectroscopy method (BDS) was applied. The BDS measurements were performed using Novocontrol Spectroscopy Alpha-A analyzer (Montabaur, Germany) at room temperature (25 °C) over a frequency range of $10^0 < f\,(\mathrm{Hz}) < 10^6$ with an applied voltage of 1 Vrms. BDS spectra were presented for phase angle (θ_0). For dielectric measurements, the samples were molded directly into printed circuit board (PCB) sandwich structures. Two PCB boards are separated by two polymer spacers of 0.33 mm thickness each (Pacoplus 4500, Pacothane, Winchester, USA) with a central hole of 38 mm diameter (Fig. 2).

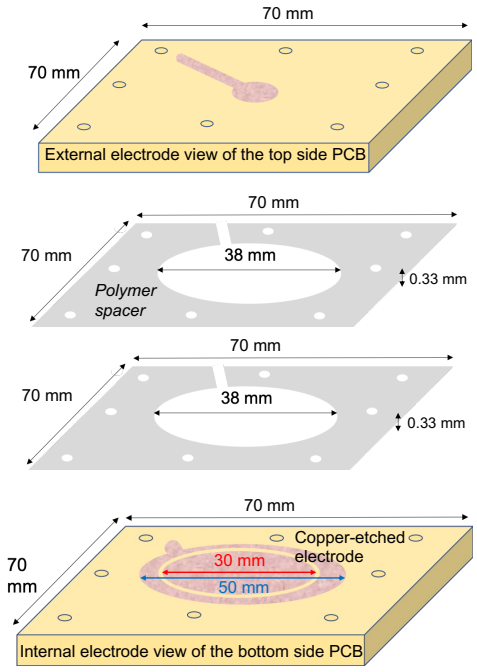

Fig. 2. Schematic representation of a printed circuit board (PCB) sandwich structure.

In the closed state, the sandwich structure contains an internal cavity of 38 mm diameter and 0.66 mm thickness, which holds the silicone during cross-linking at 80 °C. The top side PCB board presents an internal 50 mm diameter copper-etched electrode. The bottom side PCB board presents an internal 30 mm diameter electrode with a guard ring (of 50 mm outer

diameter) (as shown in Fig. 2). Metallized vias through the PCB boards extended the internal electrodes to the exterior of the sandwich structures for electrical measurements.

Micrographs of the surfaces of the neat polymer matrices and DWCNTs/silicone nanocomposites were obtained using a scanning electron microscope (TESCAN VEGA3, Czech Republic) with an accelerating voltage of 20 or 10 kV. Morphological analysis of images was performed to determine the distribution and size of nanofiller inclusions. The surface of the polymer samples was covered previously with a gold–palladium (Au/Pd) layer about 10 nm thick on the study side by sputtering for 2 min using a Q 15OR ES plus equipment (with a current of 40 mA) to make their surface conductive. The sides of the studied samples were covered with silver paint.

Estimating surface roughness is very important for many fundamental problems, including electric current conduction [17]. The topography and surface roughness of the fabricated elastomeric samples were quantitatively investigated using a Laser Scanning Confocal Microscope (VK-X series, KEYENCE, Deutschland GmbH), equipped with a ×5 (NA 22.5) objective. The samples were placed one at a time under the microscope in laboratory conditions. The light source was a green LED (661 nm), a brightfield objective and the confocal mode were also used. The procedure was performed on three different sites of the top surface on each sample. The sampling area was 800 µm × 800 µm. Based on the 3D surface profiles the roughness parameters (S_a, S_q, S_{pd}) were calculated as defined in ISO 25178 standard [18] using an automated image processing software (VK-X 3000 MultiFileAnalyzer, KEYENCE). These parameters are the most commonly used parameters of surface roughness [19].

3. Results and Discussion

Fig. 3 shows a logarithmic plot of AC electrical conductivity (σ_{AC}) versus frequency for neat polymer matrices and nanocomposites filled with different weight fractions of DWCNTs. σ_{AC} electrical conductivity increases in the all frequency range at low filler-loading (0.005 – 1.0 wt.%) for both series of DWCNTs/silicone nanocomposites. At higher contents (1.5 – 2.5 wt.%), the value of σ_{AC} does not depend on frequency, and a plateau is observed when the frequency changes from 1Hz to 1MHz.

Fig. 4a shows σ_{AC} electrical conductivity at 1 Hz for both series of the DWCNTs/silicone nanocomposites *vs* DWCNTs content. The nanocomposites using the additional PDMS-20 silicone (Fig. 4*a*, *curve 2*) exhibit better electrical conductivity over the whole range of filler-loading (0.005 – 2.5 wt.%) compared to S184 silicone alone (Fig. 4*a*, *curve 1*). Especially, as focused in Fig. 4*a* (inset), the nanocomposite with 0.05 wt.% DWCNTs based on (S184 + PDMS-20) silicones demonstrated an electrical conductivity of ~10^{-9} S/cm, while the S184-based nanocomposite had a σ_{AC} an order of magnitude lower (σ_{AC} = 10^{-10} S/cm). Furthermore, Fig. 4*a* shows that EPC, at which electrical conductivity increases sharply, is clearly observed for both series at DWCNTs content below 0.1 wt.%. Fig. 4*b* presents the impedance phase shift at 1 Hz *vs* the DWCNTs content. EPC is also visible (content at which θ_0 arises from -90° to 0°), below 0.1 wt.% for both series of samples. Fig. 4*b* further indicates a lower EPC for (S184 + PDMS-20) based samples.

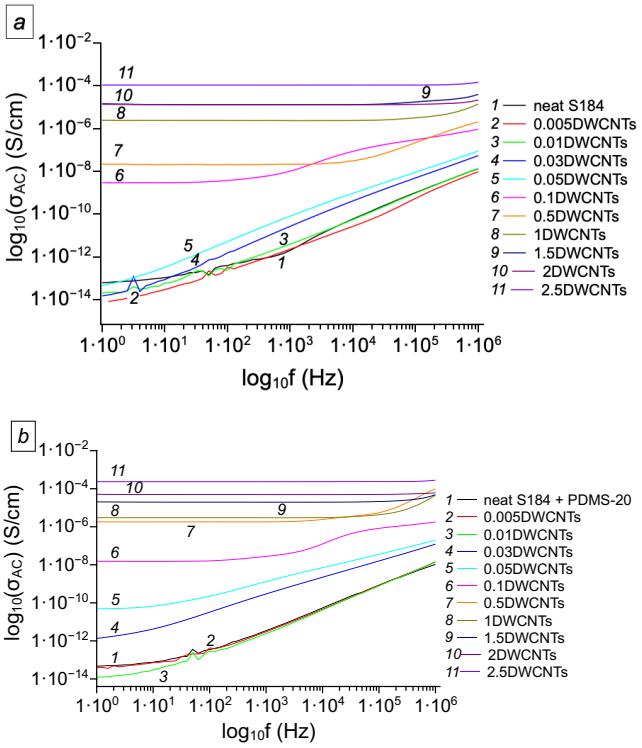

Fig. 3. Variation of AC electrical conductivity with frequency, for the different DWCNTs contents based on (*a*) S184 and (*b*) (S184 + PDMS-20) silicone matrices.

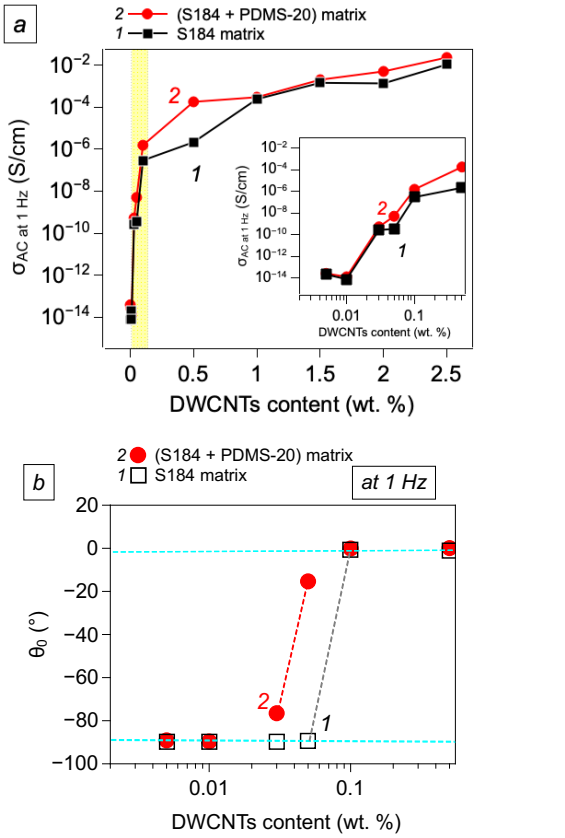

Fig. 4. (*a*) Electrical conductivity (σ_{AC}) at 1 Hz *vs* DWCNTs content for both studied DWCNTs/silicone nanocomposites. The inset shows a log–log plot for the yellow box part, where the percolation threshold occurs; (*b*) Phase shift (θ_0) of the impedance response for both silicone-based nanocomposites *vs* DWCNTs content at 1 Hz.

SEM study was applied to explore the surface morphology. The surface SEM images of neat silicones and polymer nanocomposites are presented in Fig. 5. We assume that for the same DWCNTs concentrations, the regularity of the surfaces is directly related to the dispersion state. The presented SEM images of 2.5 wt.% DWCNTs dispersed in silicone matrices (Fig. 5*c*,*d*) were representative of other observations made across the entire surface. In this scale, the DWCNTs show signs of agglomeration (Fig. 5*c*,*d*), and better dispersion in the case of adding PDMS-20 to S184 matrix (Fig. 5*d*). It is also observed that the surface of the 2.5DWCNTs/S184 nanocomposite exhibits an irregular topology with different dimensions of DWCNTs agllomerates.

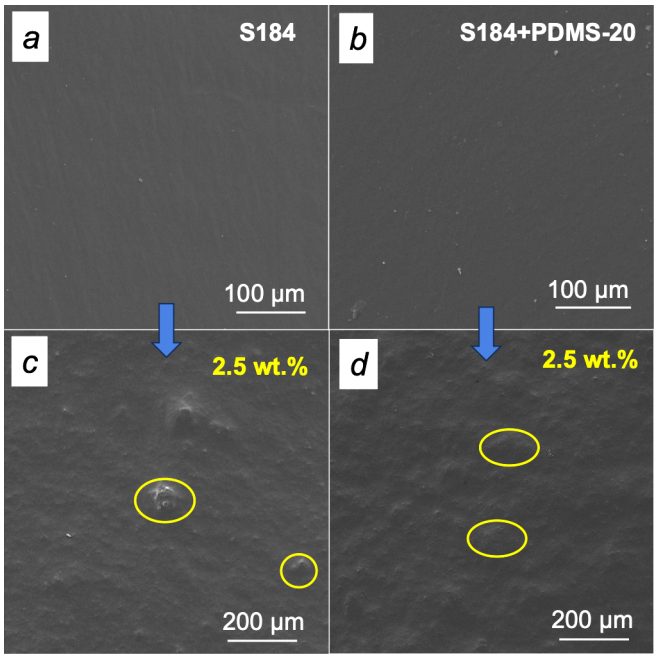

Fig. 5. SEM images of top-view for neat silicone matrices (×500, *a*,*b*) and polymer nanocomposites filled with 2.5 wt.% DWCNTs (×200, *c*,*d*). Yellow circles indicate what we assume to be DWCNTs agglomerations.

Fig. 6 shows images of the surfaces of the neat silicone matrices and polymer nanocomposites filled with 2.0 wt.% DWCNTs obtained by confocal microscopy.

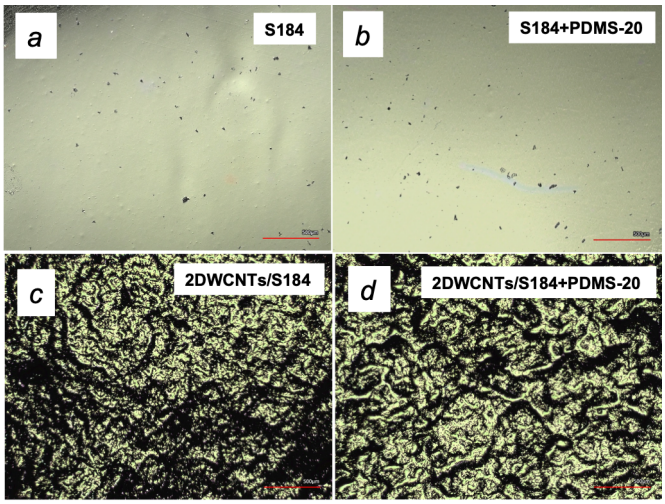

Fig. 6. Optical surface micrographs of neat silicone matrices (*a*,*b*) and polymer nanocomposites filled with 2.0 wt.% DWCNTs (*c*,*d*) with ×5 and 500 µm resolution.

Representive 3D surface profiles of selected samples are shown in Fig. 7. Table 1 presents the mean roughness parameters and standard deviations (s.d.). It can be seen (qualitatively) in Fig. 7 and Table 1 that the surface roughness values (S_a and S_q) of neat silicone matrices increased with 2 wt.% DWCNTs loading. From the other hand, the roughness (S_a) of neat S184 decreased from 15.8±2.1 µm to 7.2±1.4 µm after the addition of PDMS-20 silicone, respectively. It shoud be noted that the optical microcsopy images (Figs. 6,7) of the 2DWCNTs/S184+PDMS-20 sample illustrate more surface smoothing compared to the 2DWCNTs/S184 one. From the qualitative assessment (Table 1), it can be seen that the average values of surface roughness S_a and S_q are higher for the nanocomposite based on the silicone matrix S184.

Table 1. The average surface roughness values (±s.d.) of the neat silicone matrices and DWCNTs/silicone nanocomposites.

Sample	S_a (µm)	S_q (µm)	S_{pd} (1/mm^2)
neat S184	15.8±2.1	18.5±2.3	220±71
neat (S184 + PDMS-20)	7.2±1.4	8.6±1.4	555±251
2DWCNTs/S184	26.2±1.9	33.3±2.3	6163±126
2DWCNTs/S184+PDMS-20	22.2±0.7	28.8±0.7	6132±235

[a] ***S_a*** *– arithmetical mean height, it expresses, as an absolute value, the difference in height of each point compared to the arithmetical mean of the surface;* ***S_q*** *– root mean square height that represents the root mean square value of ordinate values within the defined area;* ***S_{pd}*** *– density of peaks that represents the number of peaks per unit area.*

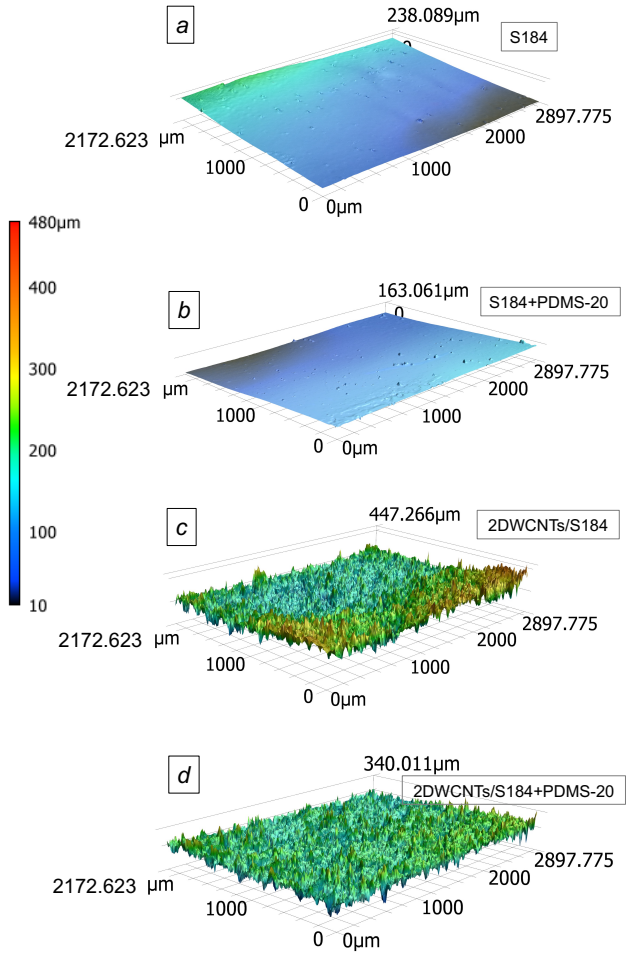

Fig. 7. 3D images obtained for neat silicone matrices (*a*,*b*) and polymer nanocomposites filled with 2.0 wt.% DWCNTs (*c*,*d*).

4. Conclusions

Electrical percolation threshold for silicone-based nanocomposites containing DWCNTs was observed below 0.1 wt.% (0.045 vol.%). Moreover, adding PDMS-20 to the S184 allowed to further decrease the EPC below 0.05 wt.% (0.022 vol.%). The presence of DWCNTs agglomerates was detected in both series of DWCNTs/silicone nanocomposites by confocal microscopy and SEM. However, changes in the surface topology resulting from the addition of a lower viscosity silicone to the S184 matrix are clearly illustrated in this study. Overall, the σ_{AC} conductivity of the nanocomposites containing PDMS-20 showed higher values. Based on surface observations performed using SEM and confocal microscopy, we assume that a better dispersion of DWCNTs in the (S184 + PDMS-20) matrix contributes to the electrical percolation threshold and the overall conductivity of the polymer nanocomposites. Further studies will be needed to understand the relationship between the observed percolation threshold and the particle-to-matrix interactions from one hand. From another hand, the potential interest of such the silicone-based nanocomposites, containing DWCNTs below the percolation threshold content, will have to be determined regarding high voltage electrical insulation systems performance enhancement.

5. Acknowledgments

This work is funded by the French national research agency under the project CARBO2DERM (grants ANR-19-CE09-0007 and ANR-23-PAUK-0080). The authors also thank GDR SEEDS CNRS for financial support.

6. References

[1] G. Sumithra, R. N. Reddy, G. Dheeraj Kumar, S. Ojha, G. Jayachandra, and G. Raghavendra, 'Review on composite classification, manufacturing, and applications', *Materials Today: Proceedings*, p. S2214785323025725, May 2023, doi: 10.1016/j.matpr.2023.04.637.

[2] R. Hsissou, R. Seghiri, Z. Benzekri, M. Hilali, M. Rafik, and A. Elharfi, 'Polymer composite materials: A comprehensive review', *Composite Structures*, vol. 262, p. 113640, Apr. 2021, doi: 10.1016/j.compstruct.2021.113640.

[3] J. P. Greene, '12 - Polymer Composites', in *Automotive Plastics and Composites*, J. P. Greene, Ed., in Plastics Design Library. , William Andrew Publishing, 2021, pp. 191–222. doi: 10.1016/B978-0-12-818008-2.00007-6.

[4] I. O. Oladele, L. N. Onuh, S. Siengchin, M. R. Sanjay, and S. O. Adelani, 'Modern Applications of Polymer Composites in Structural Industries: A Review of Philosophies, Product Development, and Graphical Applications', doi: 10.14416/j.asep.2023.07.003.

[5] S. C. Shit and P. Shah, 'A Review on Silicone Rubber', *Natl. Acad. Sci. Lett.*, vol. 36, no. 4, pp. 355–365, Aug. 2013, doi: 10.1007/s40009-013-0150-2.

[6] Q. Zhu, Z. Wang, H. Zeng, T. Yang, and X. Wang, 'Effects of graphene on various properties and applications of silicone rubber and silicone resin', *Composites Part A: Applied Science and Manufacturing*, vol. 142, p. 106240, Mar. 2021, doi: 10.1016/j.compositesa.2020.106240.

[7] S. Gilak Hakimabadi, M. Ehsani, and M. Esfandeh, 'Polymeric composites and hybrids for high-voltage insulators', *Polymer-Plastics Technology and Materials*, vol. 63, no. 7, pp. 857–871, May 2024, doi: 10.1080/25740881.2024.2307343.

[8] D. R. Paul and J. E. Mark, 'Fillers for polysiloxane ("silicone") elastomers', *Progress in Polymer Science*, vol. 35, no. 7, pp. 893–901, Jul. 2010, doi: 10.1016/j.progpolymsci.2010.03.004.

[9] N. Bitinis, M. Hernandez, R. Verdejo, J. M. Kenny, and M. A. Lopez-Manchado, 'Recent Advances in Clay/Polymer Nanocomposites', *Advanced Materials*, vol. 23, no. 44, pp. 5229–5236, 2011, doi: 10.1002/adma.201101948.

[10] J. Chen, B. Liu, X. Gao, and D. Xu, 'A review of the interfacial characteristics of polymer nanocomposites containing carbon nanotubes', *RSC Adv.*, vol. 8, no. 49, pp. 28048–28085, Aug. 2018, doi: 10.1039/C8RA04205E.

[11] M. H. Al-Saleh, 'Influence of polymer structure on the electrical resistivity of nanocomposite materials', *Synthetic Metals*, vol. 265, p. 116409, Jul. 2020, doi: 10.1016/j.synthmet.2020.116409.

[12] I. Sulym *et al.*, 'Electrical Characteristics and Surface Topography of Elastomeric Nanocomposites Based on Multi-walled Carbon Nanotubes and Poly(Dimethylsiloxane)', in *2024 IEEE 5th International Conference on Dielectrics (ICD)*, Jun. 2024, pp. 1–4. doi: 10.1109/ICD59037.2024.10613199.

[13] W. Bauhofer and J. Z. Kovacs, 'A review and analysis of electrical percolation in carbon nanotube polymer composites', *Composites Science and Technology*, vol. 69, no. 10, pp. 1486–1498, Aug. 2009, doi: 10.1016/j.compscitech.2008.06.018.

[14] A. Bassil *et al.*, 'Spectroscopic detection of carbon nanotube interaction with amphiphilic molecules in epoxy resin composites', *Journal of Applied Physics*, vol. 97, no. 3, p. 034303, 2005, doi: 10.1063/1.1846136.

[15] H. Ding *et al.*, 'Enhanced field emission properties of screen-printed doubled-walled carbon nanotubes by polydimethylsiloxane elastomer', *Applied Surface Science*, vol. 256, no. 22, pp. 6596–6600, Sep. 2010, doi: 10.1016/j.apsusc.2010.04.054.

[16] E. Flahaut, R. Bacsa, A. Peigney, and C. Laurent, 'Gram-scale CCVD synthesis of double-walled carbon nanotubes', *Chem. Commun.*, no. 12, pp. 1442–1443, Nov. 2003, doi: 10.1039/B301514A.

[17] E. S. Gadelmawla, M. M. Koura, T. M. A. Maksoud, I. M. Elewa, and H. H. Soliman, 'Roughness parameters', *Journal of Materials Processing Technology*, vol. 123, no. 1, pp. 133–145, Apr. 2002, doi: 10.1016/S0924-0136(02)00060-2.

[18] 'ISO 25178-2:2021(en), Geometrical product specifications (GPS) — Surface texture: Areal — Part 2: Terms, definitions and surface texture parameters'. Accessed: May 29, 2025. [Online]. Available: https://www.iso.org/obp/ui/#iso:std:iso:25178:-2:ed-2:v1:en

[19] A. Larena, F. Millán, M. Verdú, and G. Pinto, 'Surface roughness characterisation of multilayer polymer films for graphic arts applications', *Applied Surface Science*, vol. 174, no. 3, pp. 217–224, Apr. 2001, doi: 10.1016/S0169-4332(01)00179-9.